First-principles simulations of dissociated and molecular H_2 adsorption on Pd_4-cluster-functionalized carbon nanotubes

Chao Cao, Yao He, and Hai-ping Cheng
Department of Physics and Quantum Theory Project, University of Florida, Gainesville, Florida 32611, USA
(Received 4 September 2007; revised manuscript received 5 November 2007; published 17 January 2008)

First-principles simulations were performed to study the effect of hydrogen dissociation on the transport properties of Pd_4-cluster-functionalized carbon nanotubes. The band structure analysis indicates that within the diffusive region, hydrogen dissociation enhances the conductivity of Pd_4-cluster-functionalized CNTs, especially at high-coverage. In the high-coverage case, the Pd-cluster-functionalized CNT changes from a semiconductor to a conductor because of a major structural change. At medium and low coverages, the increase of conductivity is due to the reduced localization of electrons. The conductance change suggests that the system may serve as a hydrogen sensor.

DOI: 10.1103/PhysRevB.77.045412 PACS number(s): 61.46.Fg, 71.15.Mb, 73.21.Hb, 73.63.Fg

I. INTRODUCTION

Carbon nanotubes (CNTs), especially single walled carbon nanotubes, have drawn great attention since their discovery in 1991. The dependence of CNT band structure on the chirality and diameter was first explained by Hamada *et al.*[1] by calculating the graphene band structure with the tight-binding model. CNTs form conductors, narrow or moderate gap semiconductors according to their helical indices (n,m). Hence, the CNTs are considered to be potential molecular quantum wires.[2] Furthermore, functionalized CNTs have controllable band structures due to the chemical properties of different side groups and are therefore thoroughly studied for different purposes, e.g., chemical sensors, nanocatalysts, and molecular switches.[3–6]

Palladium (Pd) and Pd clusters are known to be reactive with hydrogen molecules, and the Pd bulk and surfaces have been studied as catalysts and hydrogen storage materials. The reaction paths for hydrogen dissociation on extended Pd surfaces have been examined to a great extent.[7–15] Both barrierless and finite-barrier dissociation of hydrogen has been found on all the Pd surfaces studied, and the barrier height is quite sensitive to the adsorption site and the orientation of the hydrogen molecule. In spite of the vast amount of work on surfaces, there is relatively little work on the hydrogen adsorption onto Pd clusters. In 2001, German *et al.*[16] studied hydrogen interactions with Pd_4 clusters using spin-polarized density functional theory calculations and obtained results similar to those from surface studies. The hydrogen dissociation on Pd clusters was also demonstrated experimentally to be dependent on the size of the cluster.[17]

Recently, the Pd-cluster-functionalized CNTs have become a hotspot of both theoretical and experimental works because they provide possibilities to construct new types of sensors and catalysts. Theoretically, Dag *et al.*[18] compared the adsorption and dissociation of hydrogen molecules on bare and functionalized CNTs, with the conclusion that Pd doping promotes the chemisorption of hydrogen molecules significantly compared to bare CNTs. Experimentally, several groups measured the conductance response of the Pd-doped CNTs or CNT thin films, under hydrogen environment, and the Pd-doped CNTs turned out to be a promising candidate for hydrogen sensing.[19–21] However, the physical mechanism underlying this sensing behavior remains unknown.

In this paper, we report our latest theoretical results on hydrogen adsorption onto Pd_4-cluster-functionalized CNTs. We focus on the effect of the hydrogen adsorption on the transport properties of the Pd_4-cluster-functionalized (5,5) CNTs. We examine both dissociative and molecular adsorptions, with high-, medium-, and low-density Pd_4-cluster coverages. The rest of this paper is organized as follows. In Sec. II, we briefly discuss the computational method and calculation details. In Sec. III, we present and analyze our results in the order of high, medium, and low coverages. Finally, in Sec. IV, we summarize our work.

II. METHODS AND CALCULATION DETAILS

The electronic structure and structural relaxation calculations were performed within the density functional theory[22] frame using the QUANTUM ESPRESSO package. In these calculations, a plane wave basis set, PBE exchange-correlation functional,[23] and RRKJ ultrasoft pseudopotentials[24] were employed. For Pd atoms, we used nonlinear core corrections, and the semicore *d* state was treated as a valence state. The use of ultrasoft pseudopotentials enabled us to use an energy cutoff as small as 32 Ry as basis, while the density cutoff was taken to be 400 Ry. The Brillouin zones were sampled by $1\times1\times32$, $1\times1\times16$, or $1\times1\times8$ special *k* points using the Monkhorst scheme[25] in the case of high, medium, and low coverages, respectively, and for density of states (DOS) calculations, the *k* points were chosen to be $1\times1\times512$ for high coverage and $1\times1\times256$ for the rest. To speed up the Kohn-Sham convergence, Gaussian smearing of width $\sigma=0.001$ Ry was used for electron occupations and then extrapolated to $\sigma=0$, and for the charge analysis, Löwdin's charge on individual atoms were obtained by projecting the total wave function onto the atomic orbitals and summing over the atom.

To model individual CNTs, a 40 Å supercell in the *x* and *y* directions was introduced so that interactions between two

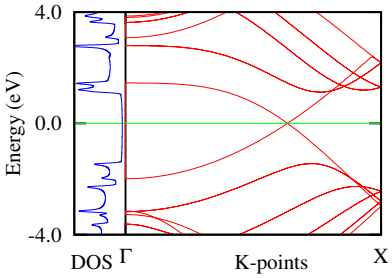

FIG. 1. (Color online) Band structure and DOS of pure (5,5) CNT. In all figures, E_F is shifted to 0.0 eV.

neighboring unit cells can be neglected. According to Ref. 16 the bond-top and bond-bond approach configurations give the most stable physisorption and chemisorption complex structures for hydrogen adsorption on Pd_4 clusters, respectively. Therefore, we use the same approach configurations for physisorption and chemisorption in our calculations. We obtain all the structures by full relaxation without any restriction on symmetry. It is well known, however, that physisorption exists only under low temperatures since the barrier from physisorption to chemisorption is very small.[14,15]

III. RESULTS AND DISCUSSION

A. Pure carbon nanotube

A pure (5,5) CNT was first modeled for comparison purposes. After optimization, we obtained a lattice constant of 2.46 Å for pure (5,5) CNT, which corresponds to a C–C bond length equal to 1.42 Å. The band structure and DOS indicate that it is a conductor (Fig. 1).

B. High coverage

The high-coverage rate was simulated with two unit (5,5) CNT doped with one Pd_4 cluster in one supercell. The fully relaxed structure is shown in Fig. 2(a). The averaged Pd–Pd bond length within one supercell is 2.67 Å and the Pd–Pd bonds across two supercells [3-2′ and 4-2′ in Fig. 2(a), i' refers to the ith Pd atom in the right nearest neighbor] have a bond length of 2.86 Å. Since CNT is a quasi-one-dimensional system, we define the palladium coverage by line coverage, i.e.,

$$\text{coverage} = \frac{\text{length covered by } Pd_4 - \text{cluster}}{\text{total length of CNT}},$$

throughout this paper. Therefore, the coverage is approximately 100% for this case. In experiments,[19,20] the number of palladium atoms per length is often even higher. Because of the doping, a radial distortion of CNT takes place and the cross section of the CNT elongates in the direction where the clusters were deposited. The whole system, however, becomes a semiconductor with a band gap of $E_g = 128$ meV [Fig. 3(a)]. Projected density of states (PDOS) analysis [Fig. 4(a)] shows that close to the Fermi energy level, the Pd clusters dominate the highest occupied band, while Pd clusters and CNT contribute roughly the same to the lowest unoccupied band. In Table I, we show Löwdin's charge of this system. The Pd_4 cluster transferred about 0.1 e to the CNT, but the total number of electrons on the carbon atoms away from the Pd cluster (i.e., the carbon atom that is not bonded with Pd cluster) was actually reduced by about 0.2. In fact, this indicates that due to the strong bonding between the carbon

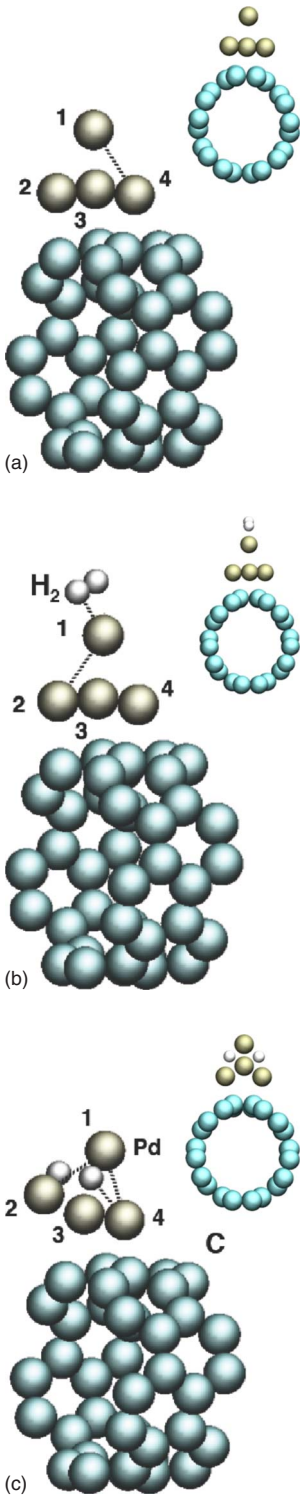

FIG. 2. (Color online) Structures for high-coverage systems. Unless otherwise specified, green atoms are carbon, white atoms are hydrogen, and gold atoms are palladium in all figures. Right-top insets are the same structures from the front view.

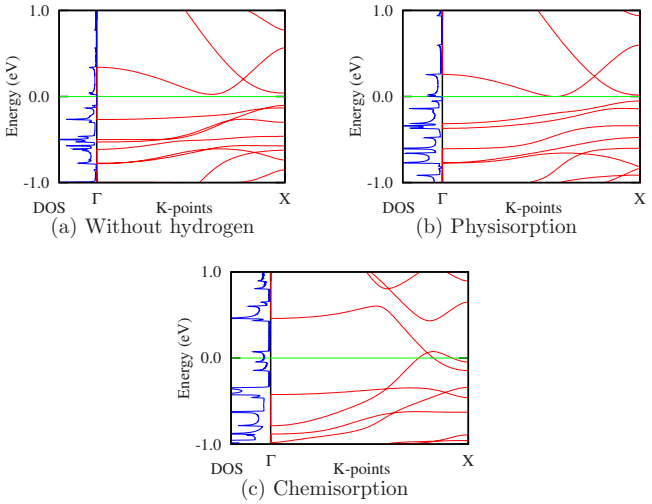

FIG. 3. (Color online) Band structure and DOS for high-coverage systems. In all figures, E_F is shifted to 0.0 eV.

and palladium atoms, localized states form at the interface between the cluster and the CNT. We show this effect by plotting the charge difference of $\rho_{\mathrm{CNT+Pd}}-\rho_{\mathrm{CNT}}-\rho_{\mathrm{Pd}}$ in Fig. 5. The electron localization opens the gap at the Fermi level.

Figures 2(b) and 2(c) illustrate the stable configuration of dissociative and molecular H_2 adsorption on this densely covered system, respectively. For both chemisorption and physisorption, the Pd–H bond lengths are 1.85 Å. The H–H distances in chemisorption and physisorption are 2.09 and 0.81 Å, respectively, comparing to the equilibrium H–H bond length of 0.75 Å in the hydrogen molecule. The binding energy is then calculated from $E_b=E_{\mathrm{CNT+Pd}}+E_{\mathrm{H_2}}-E_{\mathrm{CNT+Pd+H}}$, which turns out to be 1.06 eV for chemisorption

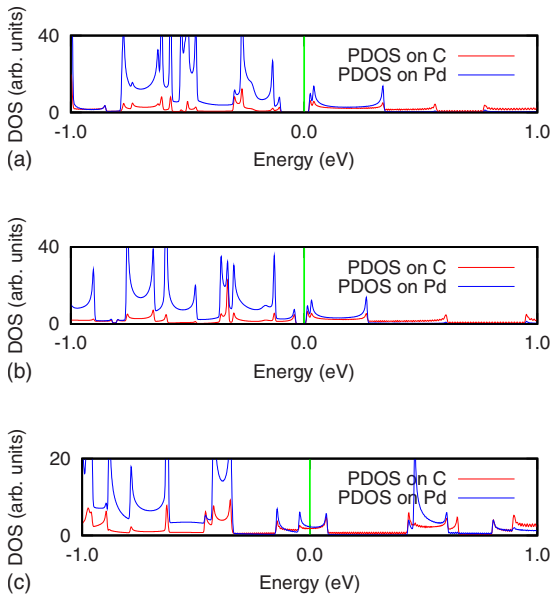

FIG. 4. (Color online) PDOS analysis for high-coverage systems. The red lines represent PDOS on carbon atoms; the blue lines represent PDOS on palladium atoms. The contributions from hydrogen atoms are negligible compared to those from C and Pd. In all figures, E_F is shifted to 0.0 eV.

TABLE I. Löwdin's charge analysis of high-coverage systems; listed numbers are scaled by the ratio of the theoretical total charge to the calculated total charge. Total C refers to all carbon atoms; C* refers to carbon atoms not bonded with palladium atoms (in pure CNT case, it is the total charge of 34 carbon atoms). Without H refers to the CNT+Pd system without hydrogen adsorption, with H_2 to the hydrogen physisorbed system, and with 2H to the hydrogen chemisorbed system.

	Pure CNT	Without H	With H_2	With 2H
Total C	160.00	160.09	160.12	160.08
C*	136.00	135.81	135.85	135.89
Total Pd		39.91	39.90	39.83
Total H			1.98	2.08

and 0.37 eV for physisorption. The molecular binding of H_2 does not significantly change the band structure nor the DOS, but the band gap is reduced from 128 to 52.1 meV [Fig. 3(b)]. In the dissociation case, however, the system was found to be a good conductor [Fig. 3(c)]. This is due to the major structural change induced by the chemisorption of hydrogen, and as a consequence, the Pd clusters form an atomic wire. In this situation, the Pd–Pd bond lengths can be classified into two categories: (1) the Pd–Pd bonds within the same *x-y* plane (a principal layer) [1-4, 4-3, and 3-1 in Fig. 2(c)], which have bond lengths of 2.64 Å: and (2) the interlayer Pd–Pd bonds [2-1, 3,4 and 2′-1, 3,4 in Fig. 2(c)], which are 2.93 Å. To test the stability of the high-coverage system before hydrogen adsorption, we removed the hydrogen atoms from the chemisorbed complex, in which Pd_4 clusters are distorted and form a wire, and then relaxed the geometry. Remarkably, the structure recovers to be the same before hydrogen adsorption. This reversibility shows that the structure before adsorption is highly stable and the sensing mechanism is robust.

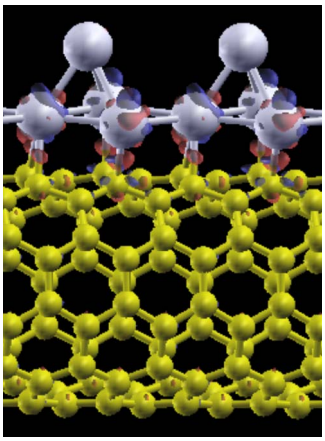

FIG. 5. (Color online) Electron localization in the CNT+Pd system calculated from $\rho_{\mathrm{CNT+Pd}}-\rho_{\mathrm{CNT}}-\rho_{\mathrm{Pd}}$: the red area indicates charge accumulation (electron localized in this area) and the blue area indicates hole accumulation. Electron localization was observed between CNT and Pd_4 cluster. In this figure, yellow atoms are carbon and white atoms are palladium.

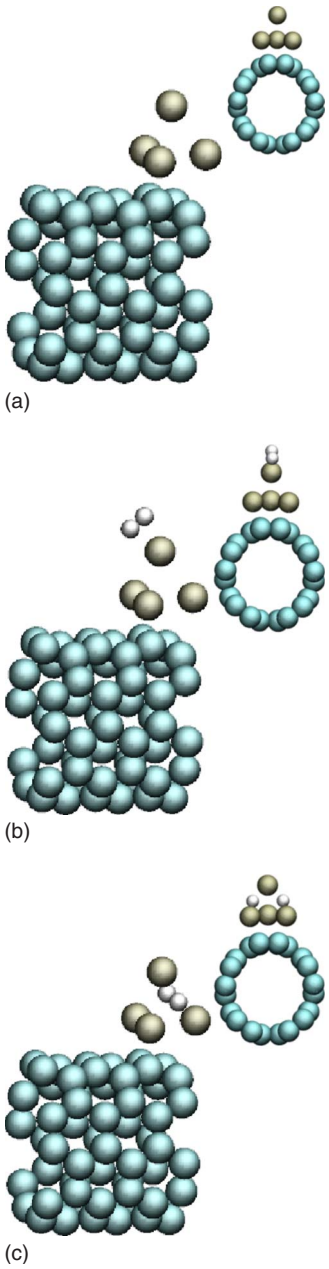

FIG. 6. (Color online) Structures for medium coverage systems. Right-top insets are the same structures from the front view.

C. Medium coverage

The medium coverage was simulated with one Pd cluster on three unit cells of CNT, which results in a 66% coverage. The relaxed Pd cluster is a perfect tetrahedron with an edge (Pd–Pd bond) length of 2.68 Å [Fig. 6(a)]. The radial distortion of the CNT, which is much less than in the high-coverage case, is also observed. Since the percentage of the carbon atoms bonded with the Pd cluster (and hence the number of localized electrons) is significantly decreased from the high-coverage case, it is expected that the medium coverage has a better conductivity. The band structure and DOS calculations [Fig. 7(a)] confirm this speculation and the finite DOS at the Fermi energy level indicates that the system

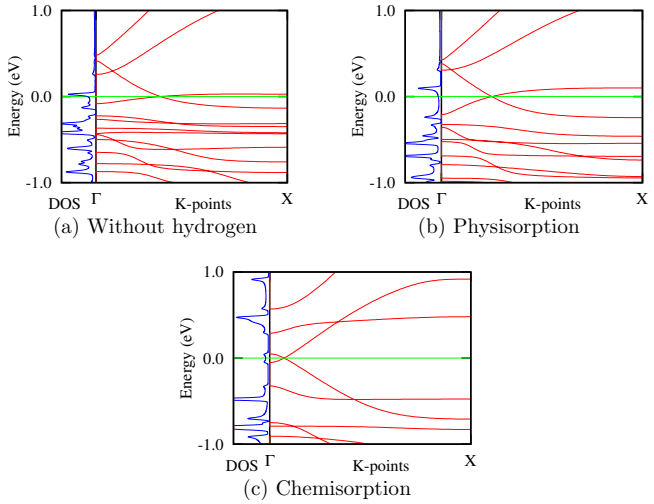

FIG. 7. (Color online) Band structure and DOS for medium coverage systems. In all figures, E_F is shifted to 0.0 eV.

is metallic. The PDOS analysis [Fig. 8(a)] shows that around the Fermi level, the Pd clusters contribute more than 60% to the total DOS, almost twice as much as the CNT does. The band structure also shows that the state contributed by the Pd cluster around the Fermi level is actually a flatband ($v_F = 3.3 \times 10^4$ m/s, the other band is 1.1×10^5 m/s), which is semilocalized; thus, the conductivity is low for this band.

The Pd–H bond lengths for the molecular and dissociative adsorptions are 1.79 and 1.82 Å, respectively, and the corresponding binding energies are 0.45 and 1.30 eV, respectively. The tetrahedron is expanded because of hydrogen adsorption. In molecular adsorption, the resulting Pd–Pd bond lengths are 2.71 Å, while in chemisorption, they are elon-

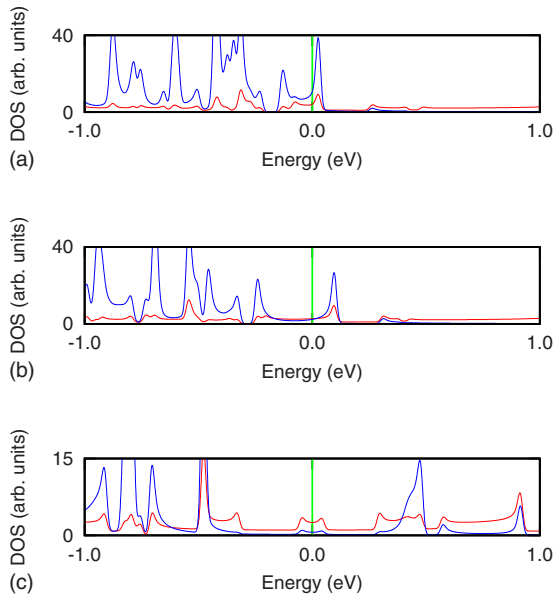

FIG. 8. (Color online) PDOS analysis for medium coverage systems. The red lines represent PDOS on carbon atoms; the blue lines represent PDOS on palladium atoms. The contributions from hydrogen atoms are negligible compared to those from C and Pd. In all figures, E_F is shifted to 0.0 eV.

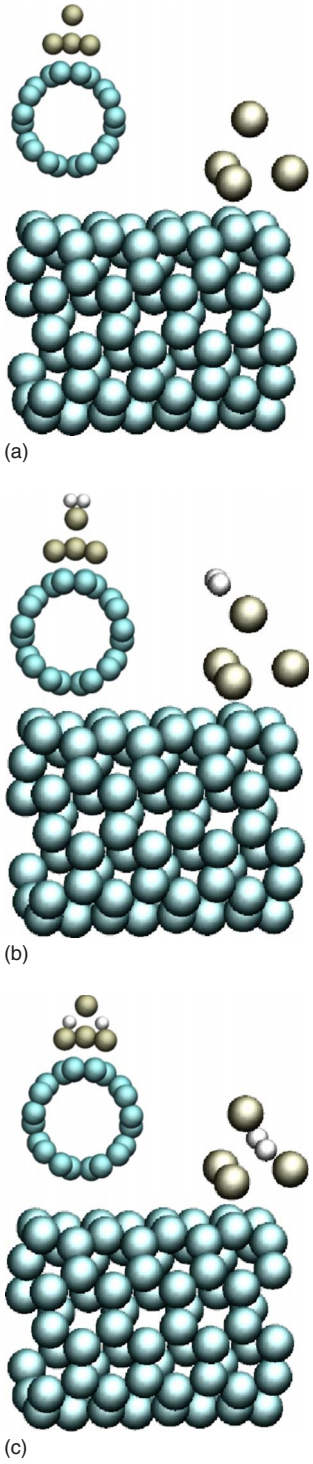

FIG. 9. (Color online) Structures for low-coverage systems. Left-top insets are the same structures from the front view.

gated to 2.81 Å [Fig. 6(c)]. However, the distance between two neighboring tetrahedrons is now much longer than in the high-coverage case; hence, the drastic structural change observed in the high coverage case no longer exists. Nevertheless, hydrogen dissociation strongly influences the electronic structure of the system. The Fermi velocities calculated from the band structure [Fig. 7(c)] are now 2.1×10^5 and 2.0×10^5 m/s, suggesting a much higher conductance in the dif-

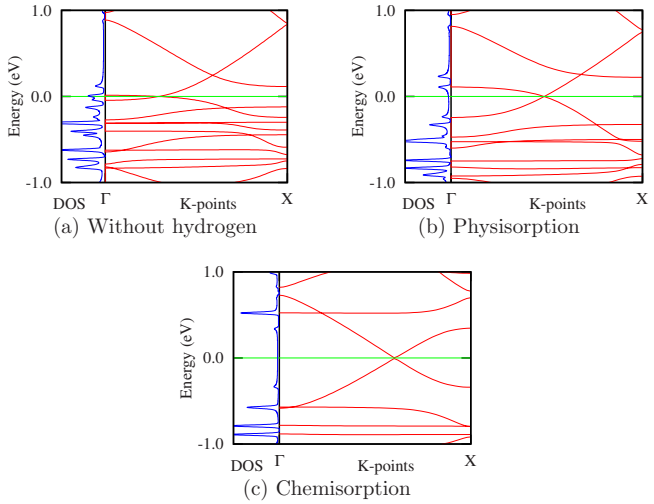

FIG. 10. (Color online) Band structure and DOS for low-coverage systems. In all figures, E_F is shifted to 0.0 eV.

fusive conducting region. Also, 80% of the DOS around E_F is contributed by CNT [Fig. 8(c)], indicating that the hydrogen dissociation on the Pd cluster reduced the localization of electrons between CNT and Pd_4 clusters. This effect is also present in physisorption, which leads to approximately equal contributions to the total DOS from the Pd clusters and the CNT [Fig. 8(b)]. The Fermi velocities in physisorption are 2.2×10^5 and 8.7×10^4 m/s [Fig. 7(b)], indicating a conductance between the system without hydrogen and chemisorption.

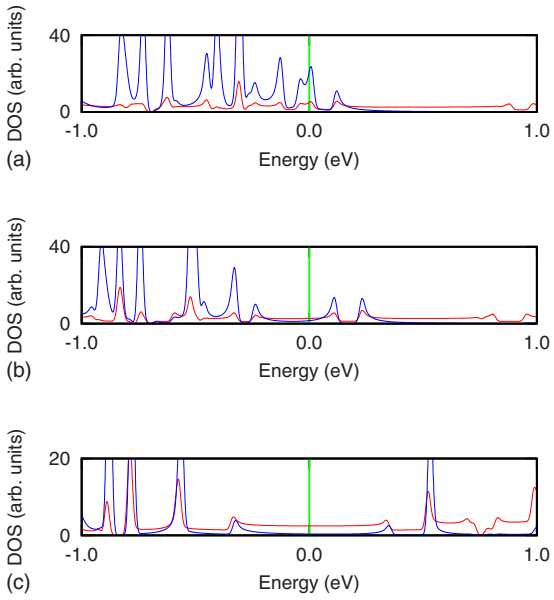

FIG. 11. (Color online) PDOS analysis for low-coverage systems. The red lines represent PDOS on carbon atoms; the blue lines represent PDOS on palladium atoms. The contributions from hydrogen atoms are negligible compared to those from C and Pd. In all figures, E_F is shifted to 0.0 eV.

D. Low coverage

Finally, we deposited one Pd_4 cluster per four unit-cell CNTs to simulate the low-coverage system. The CNT is approximately 50% covered by the Pd cluster. In this situation, the local geometry of the Pd_4 cluster is almost identical to the medium coverage case (Fig. 9). However, with even lower percentage of localized electrons than that in the medium coverage case, the system is more conducting (v_F=4.4×10^4 and 1.6×10^5 m/s) [Fig. 10(a)].

Similar to the medium coverage case, the hydrogen physisorption preserves the overall shape of the band structure around the Fermi level. It was calculated from the band structure that the Fermi velocities of the physisorbed system are 3.4×10^5 and 5.8×10^5 m/s [Fig. 10(b)], indicating a much larger electron mobility. With chemisorption, this mobility is further increased to 6.5×10^5 and 6.7×10^5 m/s [Fig. 10(c)]. PDOS analysis (Fig. 11) reveals a similar mechanism behind this conductance change, i.e., the bonding between hydrogen and palladium reduces the localization of electrons.

IV. SUMMARY AND CONCLUSION

In summary, we performed first-principles simulations on the effects of hydrogen adsorption on the electronic and transport properties of Pd_4-cluster-functionalized CNTs. A systematic change in the band-gap width versus the coverage percentage was observed, which suggests the possibility of manipulating the CNT band structure by appropriate palladium doping. Especially with 100% palladium coverage, the CNT system turns out to be semiconducting due to the electron localization effect. All the investigated systems showed an increase in conductance upon hydrogen chemisorption but the mechanisms vary: at high coverage, the adsorption of hydrogen induced a substantial structural change and the clusters formed an atomic wire; at medium and low coverage, the dissociation of hydrogen greatly reduced the localization of the binding electrons between CNT and Pd_4 clusters. The conductance change in this system suggests that the Pd-cluster-doped CNT can potentially serve as a hydrogen sensor.

ACKNOWLEDGMENTS

This work is supported by DOE under Grant No. FG02-02ER45995 and NSF through ITR-medium program. The authors want to thank DOE/NERSC, CNMS/ORNL, and the University of Florida High Performance Computing Center for providing computational resources and support that have contributed to the research results reported within this paper.

[1] N. Hamada, S. I. Sawada, and A. Oshiyama, Phys. Rev. Lett. **68**, 1579 (1992).
[2] S. J. Tans, M. H. Devoret, H. Dai, A. Thess, R. E. Smalley, L. J. Geerligs, and C. Dekker, Nature (London) **386**, 474 (1997).
[3] R. H. Baughman, A. A. Zakhidov, and W. A. de Heer, Science **297**, 787 (2002).
[4] S. J. Tans, A. R. M. Verschueren, and C. Dekker, Nature (London) **393**, 49 (1998).
[5] P. G. Collins, K. Bradley, M. Ishigami, and A. Zettle, Science **287**, 1801 (2000).
[6] J. Kong, N. R. Franklin, C. W. Zhou, M. G. Chapline, S. Peng, K. J. Cho, and H. J. Dai, Science **287**, 622 (2000).
[7] A. Gross, Surf. Sci. **363**, 1 (1996).
[8] W. Dong and J. Hafner, Phys. Rev. B **56**, 15396 (1997).
[9] A. Gross, C. M. Wei, and M. Scheffler, Surf. Sci. **416**, L1095 (1998).
[10] V. Ledentu, W. Dong, and P. Sautet, Surf. Sci. **413**, 518 (1998).
[11] M. Lischka and A. Gross, Phys. Rev. B **65**, 075420 (2002).
[12] N. Lopez, Z. Lodziana, F. Illas, and M. Salmeron, Phys. Rev. Lett. **93**, 146103 (2004).
[13] T. Mitsui, M. K. Rose, E. Fomin, D. F. Ogletree, and M. Salmeron, Nature (London) **422**, 705 (2003).
[14] P. K. Schmidt, K. Christmann, G. Kresse, J. Hafner, M. Lischka, and A. Gross, Phys. Rev. Lett. **87**, 096103 (2001).
[15] U. Muschiol, P. K. Schmidt, and K. Christmann, Surf. Sci. **395**, 182 (1998).
[16] E. D. German, I. Efremenko, and M. Sheintuch, J. Phys. Chem. A **105**, 11312 (2001).
[17] S. Y. Huang, C. D. Huang, B. T. Chang, and C. T. Yeh, J. Phys. Chem. B **110**, 21783 (2006).
[18] S. Dag, Y. Ozturk, S. Ciraci, and T. Yildirim, Phys. Rev. B **72**, 155404 (2005).
[19] J. Sippel-Oakley, H. T. Wang, B. S. Kang, Z. C. Wu, F. Ren, A. G. Rinzler, and S. J. Pearton, Nanotechnology **16**, 2218 (2005).
[20] J. Kong, M. G. Chapline, and H. J. Dai, Adv. Mater. (Weinheim, Ger.) **13**, 1384 (2001).
[21] I. Sayago, E. Terrado, E. Lafuente, M. C. Horrillo, W. K. Maser, A. M. Benito, R. Navarro, E. P. Urriolabeitia, M. T. Martinez, and J. Gutierrez, Synth. Met. **148**, 15 (2005).
[22] W. Kohn and L. Sham, Phys. Rev. **140**, 1133 (1965).
[23] J. P. Perdew, K. Burke, and M. Ernzerhof, Phys. Rev. Lett. **77**, 3865 (1996).
[24] A. M. Rappe, K. M. Rabe, E. Kaxiras, and J. D. Joannopoulos, Phys. Rev. B **41**, 1227 (1990).
[25] H. J. Monkhorst and J. D. Pack, Phys. Rev. B **13**, 5188 (1976).